Nonlinear strength quantifier based on phase correlation

Article *in* Physica A: Statistical Mechanics and its Applications · November 2019

DOI: 10.1016/j.physa.2019.123492

3 authors, including:

Yu Huang
Peking University
7 PUBLICATIONS **10** CITATIONS
SEE PROFILE

Zuntao Fu
Peking University
181 PUBLICATIONS **3,243** CITATIONS
SEE PROFILE

ARTICLE IN PRESS

Physica A xxx (xxxx) xxx

Contents lists available at ScienceDirect

Physica A

journal homepage: www.elsevier.com/locate/physa

Nonlinear strength quantifier based on phase correlation

Zhongde Yu, Yu Huang, Zuntao Fu *

Lab for Climate and Ocean-Atmosphere Studies, Department of Atmospheric and Oceanic Sciences, School of Physics, Peking University, Beijing, 100871, China

ARTICLE INFO

Article history:
Received 26 April 2019
Received in revised form 21 October 2019
Available online xxxx

Keywords:
Fourier transform
Phase correlation
Nonlinear strength quantifier
Nonlinear time series

ABSTRACT

Distinguishing linear series from nonlinear ones is of great importance, for not only understanding the processes generating these series but also their modeling and prediction. There are many methods and their nonlinear quantifiers to reach this goal, but no one is powerful enough to deal with any given series. In this study, the artificially generating series with given tailored phase correlation strength is applied to test the performance of some widely used methods and their nonlinear quantifiers given in the previous studies, both advantages and shortcomings are shown for these methods and their nonlinear metrics. Especially, spurious results from these methods and their nonlinear metrics can be found for some cases (much weak or strong phase correlations). In order to avoid these spurious results, modified phase correlation quantifiers are proposed. At the same time, multiple stripes found in the phase map can be explained from the view point of enhanced nonlinear strength.

1. Introduction

Distinguishing linear series from nonlinear ones is of great importance, for not only understanding the processes generating these series but also their modeling and prediction. For example, previous studies [1–3] show that increasing nonlinearity in time series can enhance its predictability [4–6]. In order to correctly model the nonlinear time series, nonlinear model or strategies should be adopted. By this way, higher realizable predictability can be reached [2,3]. However, if the underlying series is of linear nature, then both linear and nonlinear model/strategies work equally well. But there is much heavier computation consumption for nonlinear models or strategies compared with linear cases.

Many methods and their nonlinear quantifiers have been proposed in previous studies to quantify the nonlinear strength in a given series or distinguish the nonlinear series from the linear ones. While one of the widely used methods is magnitude or volatility correlation [7–17] based on the Detrended Fluctuation Analysis (DFA) method [18–22]. With the help of DFA, Long-Term Persistence (LTP), also called Long-Term correlation (LTC), Long-Term Memory (LTM) [23] can be well quantified in the magnitude series. However, some studies show that this magnitude correlation quantifier can work well only when the series' LTM strength is higher, such as higher than 0.75, otherwise spurious magnitude correlation will be reached [22]. At the same time, another widely used method is Multi-Fractal DFA (MF-DFA) [24], which is an extension of DFA method. The nonlinear quantifier from MF-DFA is the multi-fractal strength calculated from a given series [25–28]. Same as magnitude correlation quantifier, multi-fractal strength is only a sufficient condition for nonlinear series, rather than necessary condition. Previous study [11] has found that correlated volatility does not necessarily imply multifactality, which is in clear contradiction to the earlier hypothesis [9] that volatility correlation can infer multifactality. Both mono-fractal and multi-fractal series can be nonlinear.

* Corresponding author.
E-mail address: fuzt@pku.edu.cn (Z. Fu).

https://doi.org/10.1016/j.physa.2019.123492
0378-4371/

Please cite this article as: Z. Yu, Y. Huang and Z. Fu, Nonlinear strength quantifier based on phase correlation, Physica A (2019) 123492, https://doi.org/10.1016/j.physa.2019.123492.

Apart from these DFA-based nonlinear strength quantifiers, there are still other three common metrics. The first one is called Residual Delayed Map (RDM), developed by Sugihara and his colleagues [29]. If there are well-defined structures in residual series, which is difference between original series and its linear prediction model output, the underlying series will be nonlinear [29,30]. The second nonlinear metric is the time series irreversibility for a given series [31–36]. Unfortunately, both RDM and time series irreversibility quantifiers can work well only for some specific kinds of nonlinear series (for example, long ship waves are highly nonlinear and they have dominated RDM structures but they are not irreversible), so they can only be taken as a sufficient condition for nonlinear series.

The latest but also the most general definition of nonlinearity in time series is phase correlation [37–39]. It is thought that for a given nonlinear series, its Fourier phase series from Fourier analysis code all the nonlinear information [40–42]. For a linear series, its Fourier phases will randomly distributed in phase map. On the contrary, the nonrandom distribution in the phase map indicates the presence of nonlinearity in the underlying series [37–42]. Taking this into account, both linear and nonlinear surrogates can be artificially generated [37,38,40–43]. Accordingly, we can quantify the nonlinear strength from the phase series. For example, Pearson correlation coefficient has been taken to be an index to measure the nonlinear strength of nonlinear series from its phase series and phase map [37–39]. How well will this nonlinear strength quantifier work? If it does not work well in some cases (much weak or strong phase correlations), can we further improve the quantifier for phase correlation? What is the association between the structure in phase series (for example multiple stripes in phase map) and the nonlinear strength in the underlying time series? In this study, we will answer these questions by investigating the time series with marked nonlinear features: (i) the artificially generated time series with tailored phase correlation; (ii) the time series of economic indices with dominated nonlinear features (especially when finance crises happened) [39,44–47].

2. Data and methods

2.1. Data

2.1.1. Artificially generated series with tailored phase correlation

For a given piece of series $\{x(j)\}, j = 1, 2, 3, \ldots\ldots, N$ with data length N. The Fourier transform (FT) of the corresponding series can be written as

$$X(k) = \mathrm{FT}[x(j)] = |A(k)|\, e^{i\theta(k)}, i = \sqrt{-1} \tag{1}$$

For linear time series, the phases are uncorrelated and uniformly distributed in the interval $\theta(k) \in [-\pi, \pi]$. It is thought [37–41] that nonlinearity is coded in the phase series $\{\theta(k)\}, k = 1, 2, \ldots, \mathrm{N}/2$. At the same time, previous studies [37,40–42] show that surrogates can be generated when phases are randomized or tailored. So the time series can be generated with tailored phase correlations by inverse Fourier transform (IFT) when the phase series $\{\theta(k)\}$ are controlled [37]. If there is dominated short-range correlation in the phase series, then the phases $\theta(k)$ can be determined by

$$\theta(k+1) = a\theta(k) + \varepsilon_k(0, \sigma) \tag{2}$$

where a is the phase correlation strength, and $\varepsilon_k(0, \sigma) \in [-\pi, \pi]$ is the normally-distributed random perturbation with zero mean and standard deviation σ. By altering the phase correlation strength a in Eq. (2), we can generate time series with tailored nonlinearities by IFT to Eq. (1), i.e.

$$x(j) = \mathrm{IFT}\left[|A(k)|\, e^{i\theta(k)}\right] \tag{3}$$

In this study, we will first generate a piece of Gaussian noise with zero mean and unit standard deviation with data length $N = 20000$. Then this noise series is Fourier transformed (Eq. (1)) to achieve amplitudes and phases in frequency domain. Keep the achieved amplitudes unchanged and replace the phases with tailored phases given by Eq. (2), the time series with tailored phase correlations can be generated by Eq. (3). Thereafter, the phases from Eq. (2) are denoted as tailored phases $\theta_{Tailored}(k)$ and the phases from Eq. (1) as Fourier transformed phases $\theta_{FT}(k)$. Comparison the tailored phases $\theta_{Tailored}(k)$ with the Fourier transformed phases $\theta_{FT}(k)$ can answer why there are multiple stripes in phase map and its association with the nonlinear strength. At the same time, these results will guide us to define more suitable phase correlation quantifier.

2.1.2. Measured series in real world

Since there are dominated nonlinear features in economic index series [39,44–47], two economic index series publicly available are downloaded from internet. One is daily Year Treasury Constant Maturity Rate (YTCMR) $r(t)$ (https://fred.stlouisfed.org/series/DGS10/) covering from 1962/1/2 to 2018/12/13. And in order to remove the effect from non-stationarity, the corresponding log return $x(j)$ can be calculated as

$$x(j) = \ln r(t+1) - \ln r(t) \tag{4}$$

The well-known nonlinear effects in financial time series [39,44–47] are exemplified in Fig. 1, where dominated patched larger variability is shown in the return time series (Fig. 1a). The other is Microsoft Corporation (MSFT) stock prices (using Adj_Close) $r(t)$ downloaded from https://www.quandl.com/data/EOD/MSFT-Microsoft-Corporation-MSFT-Stock-Prices-Dividends-and-Splits, and they covered from 1991/9/11 to 2018/12/24. And the corresponding daily log return can be calculated by Eq. (4).

Please cite this article as: Z. Yu, Y. Huang and Z. Fu, Nonlinear strength quantifier based on phase correlation, Physica A (2019) 123492, https://doi.org/10.1016/j.physa.2019.123492.

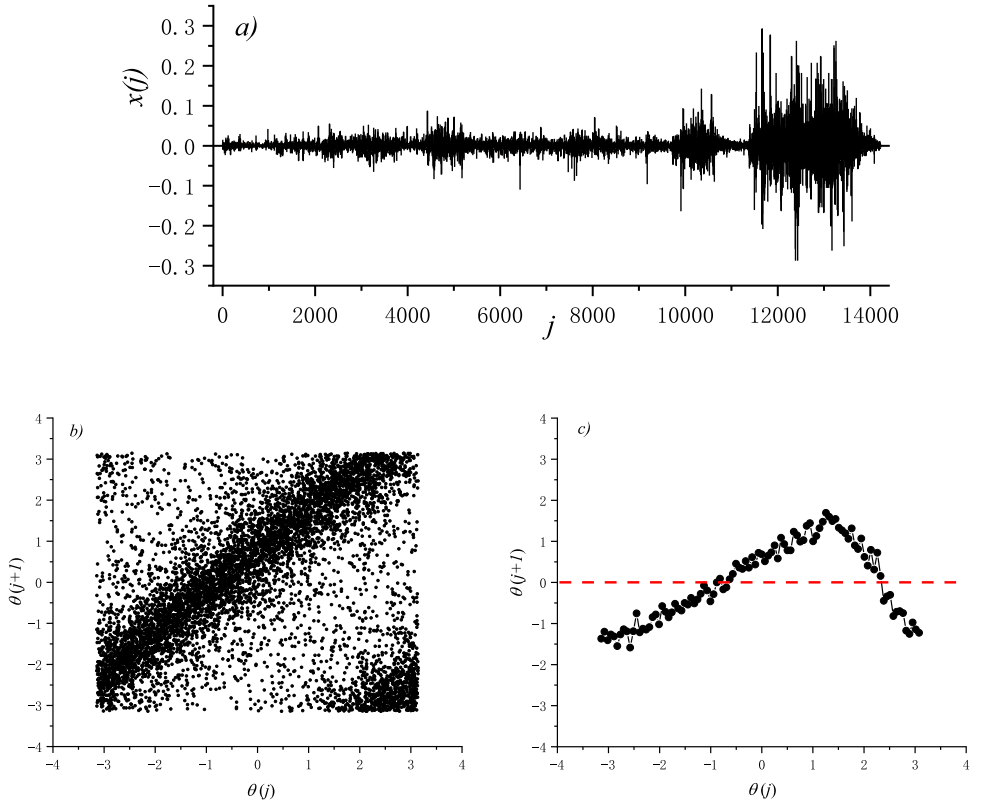

Fig. 1. (a) Log return series *x(j)* and its (b) phase map with $C(1) = 0.264$ and (c) Bin-averaged phase map of corresponding phase series for daily log return of Year Treasury Constant Maturity Rate. Here the red dash line shows the zero phase line, solid black dots and line are bin-averaged phase and black dot clouds are un-averaged phase from the Fourier transform.

2.2. Method

2.2.1. Phase correlation and quantifier

Just as previous studies [37–41] mentioned, nonlinear strength in time series can be revealed in phase series, where phase maps are sets of points $\{\theta(k+\Delta k), \theta(k)\}$ with the phase of kth FT mode and frequency delay Δ. The nonlinear strength in time series can be quantified by the Pearson correlation coefficient $C(\Delta)$ [37–39] in phase series,

$$C(\Delta) = \frac{\langle \theta(k)\,\theta(k+\Delta k)\rangle}{\sigma_{\theta(k)}\sigma_{\theta(k+\Delta k)}} \tag{5}$$

Fig. 1b shows the phase maps of YTCMR log return from Fig. 1a with $\Delta = 1$, where two marked stripes dominate the phase map and they are indicators of stronger nonlinearity. Therefore, a high Pearson correlation coefficient is reached with $C(1) = 0.264$.

2.2.2. Magnitude correlation and quantifier

Another commonly-used nonlinear quantification method is magnitude correlation based on DFA method. For given series $\{x(j)\}$, the magnitude series can be defined by two ways: one [7–17] is from the increment series $\{y(j) = |x(j+1) - x(j)|\}$, the other [12] is from the squared series $\{y(j) = x^2(j)\}$ or absolute series $\{y(j) = |x(j)|\}$. For stationary series, both ways reach nearly the same results [12]. In this study, the absolute series $\{y(j) = |x(j)|\}$ is adopted.

In order to quantify the correlation in magnitude series, DFA method can be chosen. There are three steps in the DFA algorithm:

(1) Calculate the profile of the time series

$$Y_k = \sum_{j=1}^{k} x_j, j = 1, 2, 3 \cdots\cdots, N \tag{6}$$

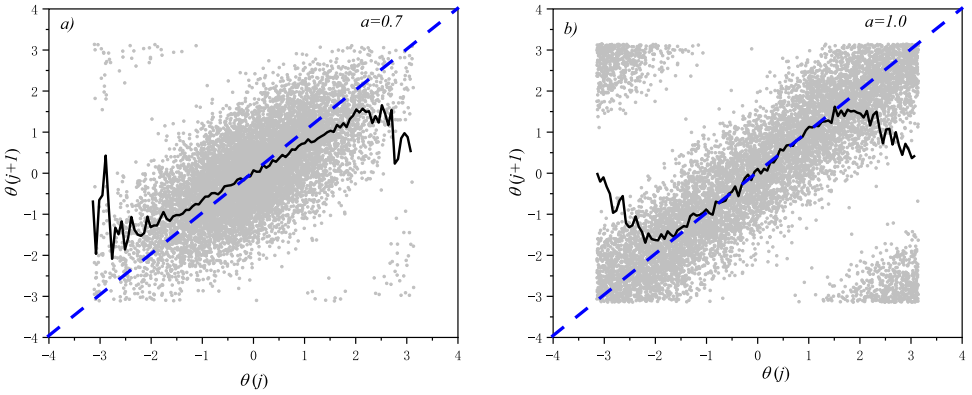

Fig. 2. The phase map and bin-averaged phase map of phase series from artificially generated series with tailored phase from Eq. (2). (a) $a = 0.7$ with $C(1) = 0.624$; (b) $a = 1.0$ with $C(1) = 0.482$. Here the blue dash line shows the 1:1 guide line, solid black dots and line are bin-averaged phase and gray dot clouds are un-averaged phase from the Fourier transform.

(2) The profile series is divided into $N_s = [\frac{N}{s}]$ non-overlapping segments with equal lengths s, indexed by $k = 1, 2, \ldots\ldots, N_s$. In each segment s, the least square regression method is applied to fit the local trend of each segment and compute the corresponding variance of the kth segment $F_s^2(k)$.
(3) Average over all segments of length s, the root-mean-square fluctuation is determined as

$$F(s) = \sqrt{\frac{1}{2N_s}\sum_{k=1}^{2N_s} F_s^2(k)} \tag{7}$$

If $F(s) \propto s^{\alpha}$, the long-range correlation strength can be accessed by the value of exponent α. Consequently, when DFA is applied to the magnitude series $\{y(j)\}$, the derived exponent α clearly different from those from Fourier phase randomization surrogates (PRS) [41,42] indicates there is nonlinearity in the original series $\{x(j)\}$ [7–17].

3. Results

3.1. Inability of magnitude and phase correlation

First of all, we check whether the previously proposed methods and nonlinear quantifiers work well when the artificially generated series with given phase correlation strength from Eq. (2) are analyzed. From Eq. (2), we know that when the correlation strength increases (the value of a in Eq. (2) increases), so does nonlinearity strength in artificially generated series through Eqs. (3) and (2) by means of IFT. However, this result cannot be well recovered by the phase correlation metric Eq. (5) as suggested in the previous studies [37–39]. Especially, this kind of failure is much more common for stronger phase correlation cases (see the results shown in Fig. 2). The phase map for two kinds of phase correlations $a = 0.7$ and $a = 1.0$ shows different results, and there are more marked multiple stripes features for case of $a = 1.0$ in Fig. 2b, so the nonlinear strength is higher for $a = 1.0$. From these two generated series by means of Eqs. (2) and (3), and the derived phase series by FT through Eq. (1), however, the calculated Pearson correlation coefficient $C(1)$ gives totally contradictive results with $C(1) = 0.482$ for $a = 1.0$ but $C(1) = 0.624$ for $a = 0.7$. This means, that the Pearson correlation coefficient $C(\Delta)$ metric in Eq. (5) [37–39] cannot always reach the correct results, and some modifications must be carried out before we can apply this metric with confidence.

The inability of magnitude correlation can be found in Fig. 3. From Fig. 1a and b, the stronger nonlinearity has been found in YTCMR log return series and its phase map. However, the magnitude correlation derived from this series is not high enough to differentiate from those from linear series, especially over the smaller scale range (see Fig. 3a, where deviation from results of PRS series is minor). This kind of inability of magnitude correlation can be further confirmed in the artificially generated series with tailored phase correlation. As presented in Fig. 2, when phase correlation exists, the nonlinearity should be revealed in the generated series with this phase correlation. However, the magnitude correlation results given in Fig. 3b show that there is no nonlinearity, since the magnitude correlations from both original and PRS series reach the same results. This result is consistent with findings in previous studies [16,17]. When the LTM strength in original series is weaker (the value of exponent α is smaller than 0.75), DFA method will reach spurious results in magnitude correlation. Actually, LTM is weaker ($\alpha = 0.5$) in the artificially generated series when the tailored phase correlation strength is $a = 0.9$.

Please cite this article as: Z. Yu, Y. Huang and Z. Fu, Nonlinear strength quantifier based on phase correlation, Physica A (2019) 123492, https://doi.org/10.1016/j.physa.2019.123492.

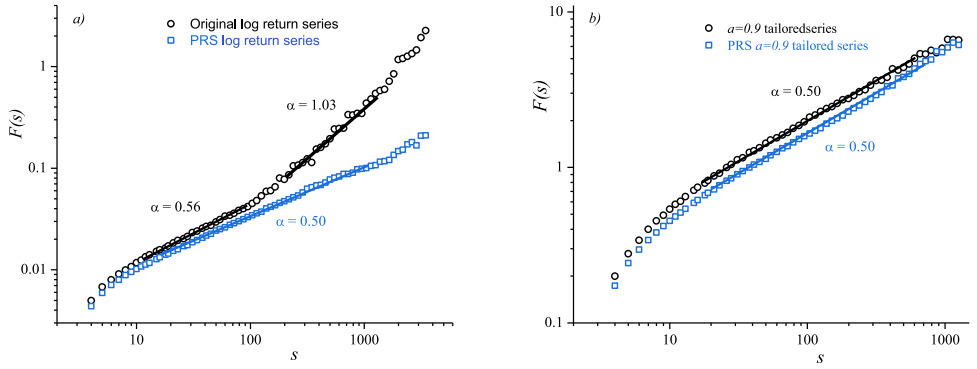

Fig. 3. DFA results for magnitude series $|x(j)|$ for original series with their PRS surrogates from different cases: (a) daily log return of YTCMR, (b) tailored series with $a = 0.9$ from Eq. (2).

3.2. Correct quantification of phase correlation: new quantifier

Since both magnitude correlation and Pearson correlation coefficient $C(\Delta)$ from the phase series cannot perform well in some cases, new nonlinear metric should be proposed. From the raw phase series, the dot cloud in phase map makes the direct quantification of nonlinear strength much difficult. To get a better pattern in phase map, insights given on RDM [29,30] can be learnt to sort and bin the phases $\{\theta(k)\}$ into groups of $M = 100$ (In fact, different bin sizes will not alter the results too much, figures not shown here), and in each bin the averaged phases $\{\theta(k+1)\}$ are reached. By this way, the systematic patterns (lines with their own features) in the bin-averaged phase map can be displayed more clearly, see Fig. 1c, where stronger nonlinearity is revealed with an upside-down "V" pattern. If there is no any nonlinearity in the underlying series, the bin-averaged phase pattern will be a line along the red dash line shown in Fig. 1c. The larger deviation from this red dash line, the stronger nonlinearity exits in the understudied series. This feature is indeed realized in the artificially generated series with tailored phase correlations, see Fig. 4. When the phase correlation is much weaker, such as $a = 0.1$, the bin-averaged phase pattern nearly collapses with the red dash line (Fig. 4a). As the strength of phase correlation increases, the deviation from this red dash line becomes larger (Fig. 4b–d). At the same time, the central part of phase pattern moves gradually toward the 1:1 diagonal line (Figs. 2a and b, 4a–d), when the phase correlation strength is $a = 1.0$, the central part of phase pattern collapses with the 1:1 diagonal line (Fig. 2b).

All above-mentioned features are subjective and qualitative, can we define an objective and quantitative estimation for this variation related to phase correlation? In RDM metric given in reference [30], bin-averaged patterns are quantified as

$$R = \sqrt{\frac{C^2(1) + C^2(2)}{2}} \tag{8}$$

where $C^2(k)$ is defined as Eq. (5), but calculated from the bin-averaged phases. In fact, just as Patil and his coauthors [30] mentioned, this quantifier does not work well for all cases and it only works well when autocorrelation structure is dominated by correlations between an arbitrary point and its four nearest neighbors [30].

In order to reach a correct quantification to phase correlation, we propose two more quantifiers related to bin-averaged phases. One is defined according to departures of bin-averaged phases from the guided red dash line, and for each bin the vertical departure distance (denoting as the pink vertical bar in Fig. 4b) and their ensemble for all bins can be quantified as

$$d = \frac{1}{M}\sum_{k=1}^{M} \left|\bar{\theta}_k\right| / D \tag{9}$$

with the possible ensemble maximum departure distance (i.e. in each bin distance from the 1:1 diagonal line to the idealized red dash line, which is denoted as the green vertical bar in Fig. 4b)

$$D = \frac{1}{M}\sum_{k=1}^{M/2} \frac{2k\pi}{M} \tag{10}$$

The other is a combination of Eqs. (8) and (9), i.e.

$$S = R \times d \tag{11}$$

Since the deviation of bin-averaged phases from the idealized red dash line is gradually increased as the phase correlation increases, quantifiers both d and S may give a better quantification of nonlinearity in given series than $C(1)$, or R.

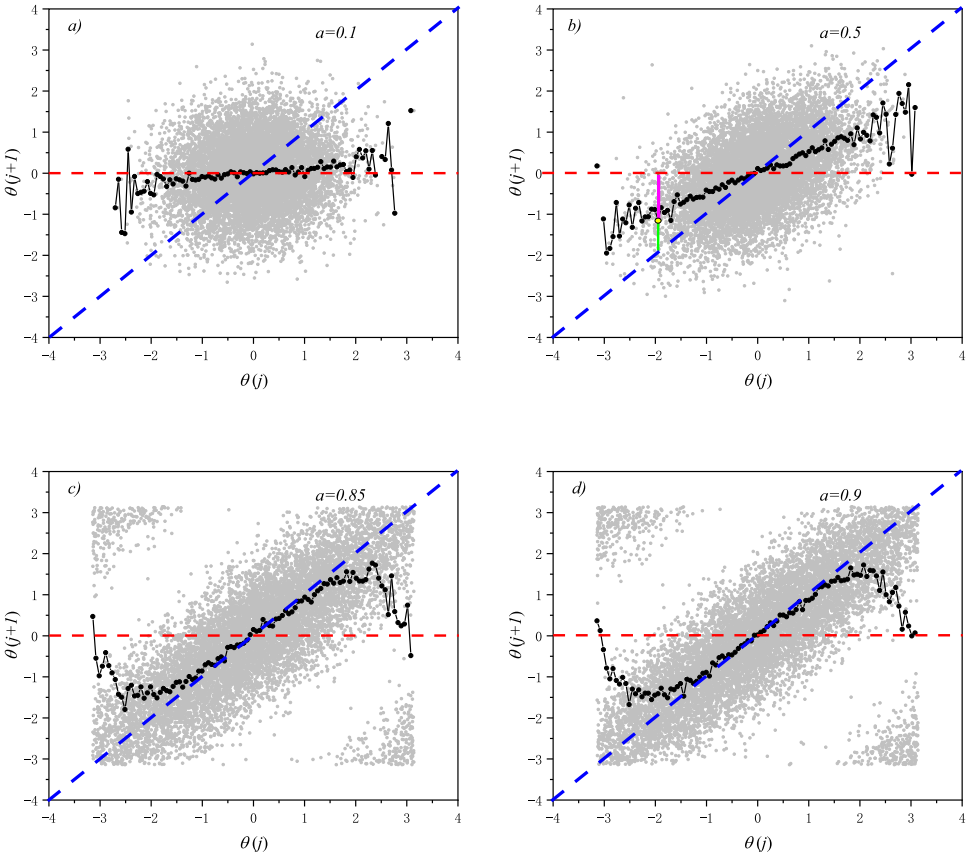

Fig. 4. The phase map and bin-averaged phase map of phase series from artificially generated series with tailored phase from Eq. (2) with different phase correlation strength. (a) a = 0.1; (b) a = 0.5; (c) a = 0.85; (d) a = 0.9. Here the blue dash line shows the 1:1 guide line, the red dash line shows the zero phase line, solid black dots and line are bin-averaged phase and gray dot clouds are un-averaged phase from the Fourier transform. The pink vertical bar and green vertical bar in Fig. 4b show the phase departure from the zero phase line.

3.3. Correspondence between nonlinearity and phase correlation

As a suitable quantifier for nonlinear strength of any given series, it should reflect the correlation variations in phase series, i.e. two aspects should be satisfied simultaneously. One is high correlation between nonlinear quantifier and phase correlation strength, which can be measured by the Pearson correlation coefficient between each nonlinear quantifier and phase correlation strength a

$$P = \frac{\langle a\,(k)\, q\,(k)\rangle}{\sigma_{a(k)}\sigma_{q(k)}} \tag{12}$$

where $q\,(k)$ can be any nonlinear quantifier among $C(1)$, R, d or S. The other is monotonic variation of nonlinear quantifier with phase correlation strength, which can be measured by the Spearman correlation coefficient between each nonlinear quantifier and phase correlation strength a

$$Sp = \frac{\langle Rank\,[a\,(k)]\, Rank[q\,(k)]\rangle}{\sigma_{Rank[a(k)]}\sigma_{Rank[q(k)]}} \tag{13}$$

where $Rank[a\,(k)]$ is the rank of $a\,(k)$ for $k = 1, 2, \ldots, 11$.

If a nonlinear quantifier performs in a more consistent way, there should be higher value for P and Sp simultaneously. We will check whether the above mentioned four phase correlation measures are able to reach this aim. Details results are shown in Fig. 5 and quantitative results for each nonlinear quantifier are summarized in Table 1, from which we can found that both d and S perform better. First of all, $C(\Delta = 1)$ only performs perfectly when phase correlation strength a is weak (smaller than 0.5), when the phase correlation strength a is stronger (larger than 0.6), $C(\Delta = 1)$ performs worse as it does not increase monotonically with the increasing phase correlation strength a. The lowest values of both P and Sp for $C(\Delta = 1)$ quantitatively reflect the worst performance of $C(\Delta = 1)$ among these four nonlinear quantifiers. Quantifier R follows the monotonic variation condition, but it correlates with phase correlation strength in a weaker way

Please cite this article as: Z. Yu, Y. Huang and Z. Fu, Nonlinear strength quantifier based on phase correlation, Physica A (2019) 123492, https://doi.org/10.1016/j.physa.2019.123492.

Table 1
Quantitative performance of each phase correlation quantifier.

	$C(1)$	R	d	S
P	0.90	0.94	0.97	0.98
Sp	0.88	1.00	1.00	1.00

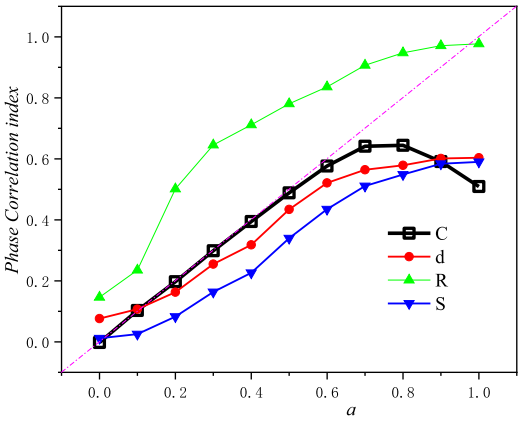

Fig. 5. Phase correlation index for given tailored phase correlation strength. Four phase correlation indices ($C(1)$ hollow squares, R up triangles, S down triangles, d solid dots) and their variations with corresponding phase correlation strength are shown. The best phase correlation quantifier should be along the 1:1 line, which changes monotonically with the phase correlation strength.

compared with both d and S (see Table 1). For smaller variation of a from 0.1 to 0.2, the change of R is abrupt (see Fig. 5). This situation will not happen for both d and S, and both of them change monotonically and highly correlates with the variations of the phase correlation. There exists one-to-one correspondence between the new nonlinear quantifiers d or S and the phase correlation a.

3.4. Cause for inability of phase correlation coefficient

At last, we want to show why the Pearson correlation coefficient of phase series does not perform well when the phase correlation a is higher than 0.5. From phase dot cloud in phase map (Fig. 4), it is obvious that when a is smaller than 0.5, there is no multiple stripes in phase map, whereas when a is larger than 0.5, the multiple stripes will appear, this feature will be more dominated when the phase correlation is much stronger. From the tailored phases given in Eq. (2), we can learn why there is so distinguished difference between weaker and stronger phase correlations. It should be noted that in Eq. (2), the random term $\varepsilon_k\,(0,\sigma) \in [-\pi, \pi]$ is keep unchanged for each case of phase correlation a. However, if the phase correlation strength a is increased beyond 0.5, then the dynamic range of the tailored phases $\theta_{Tailored}(k)$ will be altered greatly. This can be found in Fig. 6a ($a = 0.5$), the dynamic range of the tailored phases is roughly from -3.5 to 3.5, but it is roughly from -6.0 to 6.0 in Fig. 6c ($a = 0.85$). After FT, $\theta_{FT}(k)$ will be altered differently, see Fig. 6b ($a = 0.5$) unchanged for weak phase correlation strength and Fig. 6d ($a = 0.85$) changed greatly for strong phase correlation strength. More clearly, this marked difference can be found in the scatter plot between $\theta_{Tailored}(k)$ and $\theta_{FT}(k)$. For the case of $a = 0.5$, all the data points are along the 1:1 diagonal line (Fig. 6e). However, there are three lines for the case of $a = 0.85$, apart from the 1:1 diagonal line, there are other two minor lines in parallel with the 1:1 diagonal line (Fig. 6f). Higher correlations in the phase series will lead to larger variability in phases and clustering in extreme events in the phase series [48]. But the FT phase can only exist in the interval $[-\pi, \pi]$, so all phases beyond this interval will be altered. This change will lead to the multiple stripes in the phase map. In real-world series, the phases are unnecessarily in the interval $[-\pi, \pi]$, so there are often the multiple stripes in the phase map from the FT phases (see Fig. 1b).

4. Discussions and conclusions

Nonlinearity is ubiquitous in the time series observed from real-world systems, how to quantify the nonlinear strength in the understudied series is of great important. Correct quantification of nonlinear strength in series might help us distinguish the linear series from the nonlinear ones. And this classification can further guide us to choose suitable models to simulate and predict the understudied series. At the same time, deep understanding on the generating mechanisms can be reached for these series through these nonlinear quantifications. In this study, both advantages and shortcomings of the commonly-used phase correlation quantifiers in the previous studies were investigated, and two improved quantifiers were proposed. Compared with these quantifiers $C(1)$ and R, the overall performance of the new proposed quantifiers d and S are better.

Please cite this article as: Z. Yu, Y. Huang and Z. Fu, Nonlinear strength quantifier based on phase correlation, Physica A (2019) 123492, https://doi.org/10.1016/j.physa.2019.123492.

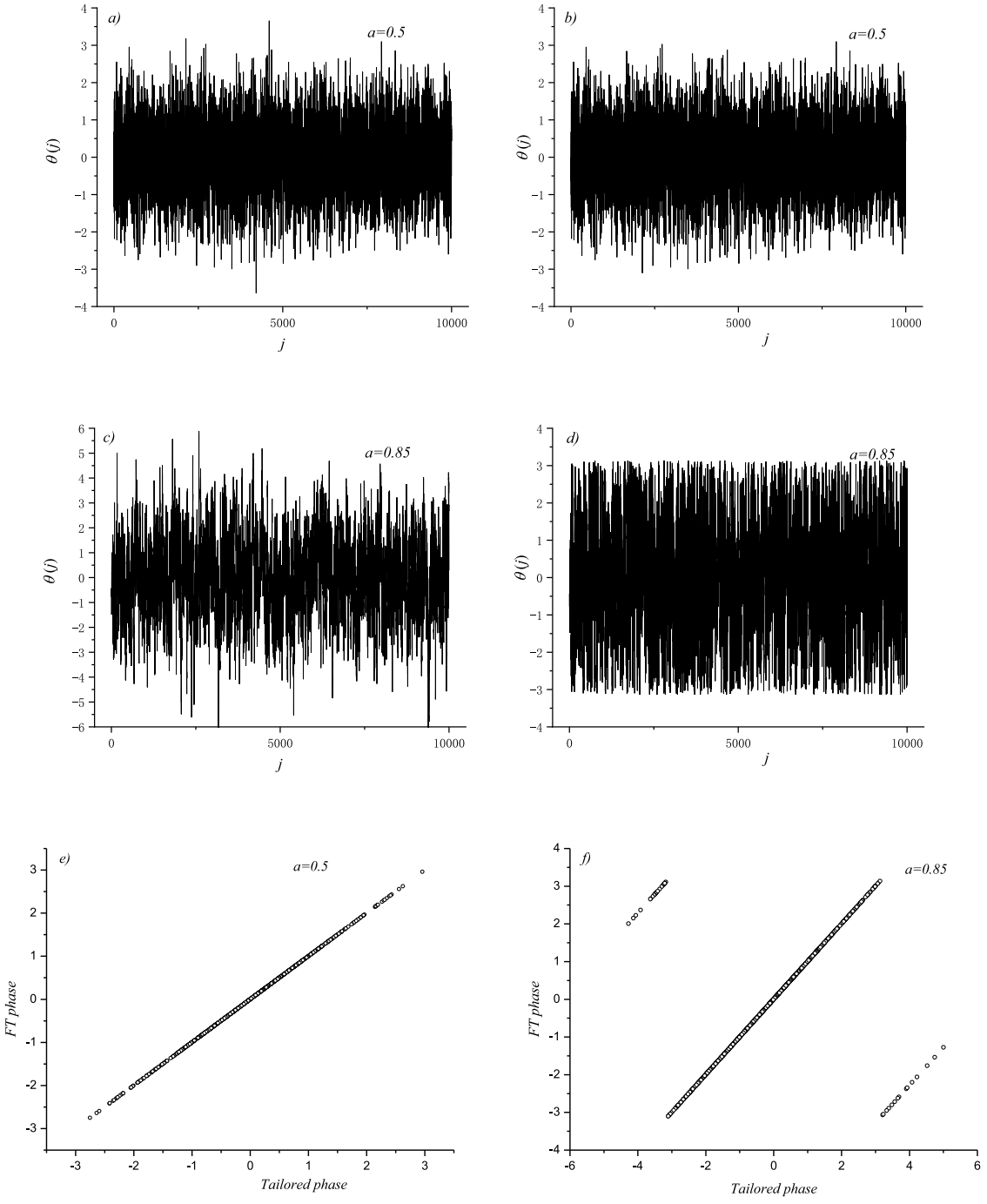

Fig. 6. The tailored phase series and its corresponding Fourier transformed phase series from artificially generated series with the tailored phase series from Eq. (2). (a) and (b) for $a = 0.5$; (c) and (d) for $a = 0.85$. (e) and (f) show the scatter plots from (a) and (b), and (c) and (d). The results show that the values of the tailored phase series will be out of the interval $[-\pi, \pi]$ when the phase correlation strength is larger than 0.5. However, the values of the transformed phase series are always within the interval $[-\pi, \pi]$ so that all values of the tailored phase series beyond the interval $[-\pi, \pi]$ will be altered (see Fig. 6d), which will lead to the multiple stripes in phase map.

For correct nonlinear quantification, the confidential interval at the given significance level should be also given. From 1000 samples of normally-distributed random series of zero mean and unit standard deviation with data length of 20 000, with the help of FT Eq. (1), 1000 samples of phase series $\theta_{FT}(k)$ can be obtained. Based on these phase series, four nonlinear quantifiers can be calculated to obtain their mean and standard deviation. The details are listed as follows

Please cite this article as: Z. Yu, Y. Huang and Z. Fu, Nonlinear strength quantifier based on phase correlation, Physica A (2019) 123492, https://doi.org/10.1016/j.physa.2019.123492.

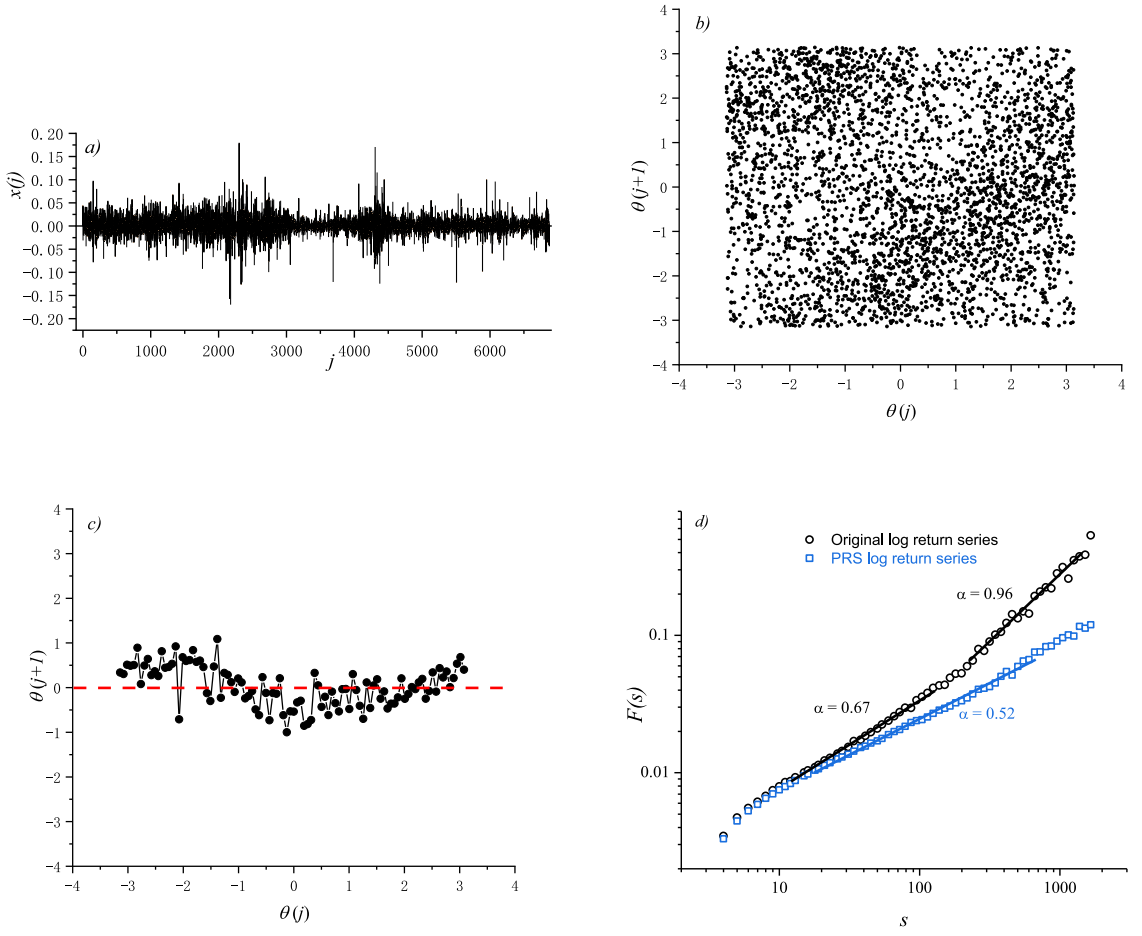

Fig. 7. (a) Log return series $x(j)$ and its (b) phase map with $C(1) = -0.079$ and (c) Bin-averaged phase map of corresponding phase series (d) DFA results for magnitude series $|x(j)|$ for daily log return of Microsoft Corporation (MSFT) stock prices their PRS surrogates.

(mean $\mp$ standard deviation). $C(1): -0.0002 \mp 0.0103$; R: 0.089 ∓ 0.045; S: 0.008 ∓ 0.004; d: 0.091 ∓ 0.007. Among them, quantifier S is the most desirable due to its smaller mean and the smallest standard deviation.

When applying the methods to real-world series, such as YTCMR series, the corresponding results are as follows: $C(1) = 0.264$; R $= 0.953$; $S = 0.496$; $d = 0.521$. Their statistical significance can be tested by 1000 reshuffling generated surrogates and details are summarized as follows: $C(1): -0.003 \mp 0.021$; R: 0.095 ∓ 0.048; S: 0.011 ∓ 0.006; d: 0.111 ∓ 0.009. The results for these four quantifiers all indicate that there exists stronger nonlinearity in YTCMR return series. For another financial (MSFT) series, detailed results are shown in Fig. 7. Compared with the results for YTCMR series, the nonlinearity in MSFT is weaker. The dot cloud in phase map (Fig. 7b) is more random, and not so easily discernable compared with those for YTCMR (Fig. 1b). However, after the bin-averaging, phase pattern is more discernable. It is obvious that there is weaker nonlinearity in MSFT return series. Detailed nonlinear quantifiers' results are as follows: $C(1) = -0.079$; R $= 0.553$; $S = 0.118$; $d = 0.214$. Their statistical significance from 1000 reshuffling surrogates are: $C(1): -0.001 \mp 0.023$; R: 0.091 ∓ 0.039; S: 0.014 ∓ 0.006; d: 0.157 ∓ 0.011. At the significance level of *99%* or above, all four nonlinear quantifiers reach the same consistent conclusion: there is significant nonlinearity in MSFT return series. Three of them suggest the nonlinearity is weak apart from R' s strong nonlinearity indication. This result is just as expected, since nonlinear quantifier R will give overestimated results when the phase correlation is weak (see Fig. 5). At last, we want to point out that magnitude correlation, which has been often used in the previous studies, may also provide overestimated nonlinearity quantification for MSFT return series (see Fig. 7d), where the estimated nonlinearity quantification for MSFT return series is higher than that in YTCMR return series (see Fig. 3a). The above results indicate that the nonlinear quantification is more complicated in real-world series than in output series from theoretical models, and results from only one nonlinear quantifier might lead to spurious conclusions.

Since nonlinearity is ubiquitous in real-world series, the applications of the proposed nonlinear quantifiers can be extended to other series in wide fields. For example, it is reported [35,49] that there are marked nonlinear features in Northern Annular Mode (NAM) variability, the variation of daily mean surface air temperature is temporal irreversible [31–34] and there are contrasting multi-fractal behaviors of diurnal temperature range over the north and the south of

China [27]. All these nonlinear features can be further tested in a more fundamental way of Fourier transformation, by means of nonlinear quantifiers given in this study.

Declaration of competing interest

The authors declare that they have no known competing financial interests or personal relationships that could have appeared to influence the work reported in this paper.

Acknowledgment

This study was supported by the National Natural Science Foundation of China through Grants (No. 41675049 and No. 41475048).

References

[1] Z. Ye, W.W. Hsieh, Enhancing predictability by increasing nonlinearity in ENSO and Lorenz systems, Nonlinear Process. Geophys. 15 (2008) 793–801.
[2] Y. Huang, Z.T. Fu, Enhanced time series predictability with well-defined structures, Theor. Appl. Climatol. (2019) http://dx.doi.org/10.1007/s00704-019-02836-6.
[3] S. Fu, Y. Huang, T. Feng, D. Nian, Z.T. Fu, Regional contrasting DTR's predictability over China, Physica A 521 (2019) 282–292.
[4] R.Q. Ding, J.P. Li, K.H. Seo, Estimate of the predictability of boreal summer and winter intraseasonal oscillations from observations, Mon. Weather Rev. 139 (2011) 2421–2438.
[5] J.P. Li, R.Q. Ding, Temporal-spatial distribution of atmospheric predictability limit by local dynamical analogues, Mon. Weather Rev. 139 (2011) 3265–3283.
[6] Z.S. Zhang, Z.Q. Gong, R. Zhi, G.L. Feng, J.G. Hu, Preliminary research on the relationship between long-range correlations and predictability, Chin. Phys. B 20 (2011) 019201.
[7] Y. Ashkenazy, P.C. Ivanov, S. Havlin, C.K. Peng, A.L. Goldberger, H.E. Stanley, Magnitude and sign correlations in heartbeat fluctuations, Phys. Rev. Lett. 86 (2001) 1900–1903.
[8] J.W. Kantelhardt, Y. Ashkenazy, P.C. Ivanov, A. Bunde, S. Havlin, T. Penzel, J.H. Peter, H.E. Stanley, Characterization of sleep stages by correlations in the magnitude and sign of heartbeat increments, Phys. Rev. E 65 (2002) 051908.
[9] Y. Ashkenazy, S. Havlin, P.C. Ivanov, C.K. Peng, V. Schulte-Frohlinde, H.E. Stanley, Magnitude and sign scaling in power-law correlated time series, Physica A 323 (2003) 19–41.
[10] Y. Ashkenazy, D.R. Baker, H. Gildor, S. Havlin, Nonlinearity and multifractality of climate change in the past 420 000 years, Geophys. Res. Lett. 30 (2003) 2146–2150.
[11] R.B. Govindan, H. Kantz, Long-term correlations and multifractality in surface wind speed, Europhys. Lett. 68 (2004) 184–190.
[12] T. Kalisky, Y. Ashkenazy, S. Havlin, Volatility of linear and nonlinear time series, Phys. Rev. E 72 (2005) 011913.
[13] I. Bartos, I.M. Jánosi, Nonlinear correlations of daily temperature records over land, Nonlinear Process. Geophys. 13 (2006) 571–576.
[14] Q. Li, Z. Fu, N. Yuan, F. Xie, Effects of non-stationarity on the magnitude and sign scaling in the multi-scale vertical velocity increment, Physica A 410 (2014) 9–16.
[15] M. Gomez-Extremera, P. Carpena, P.C. Ivanov, P.A. Bernaola-Galván, Magnitude and sign of long-range correlated time series: Decomposition and surrogate signal generation, Phys. Rev. E 93 (2016) 042201.
[16] P.A. Bernaola-Galván, M. Gómez-Extremera, A.R. Romance, P. Carpena, Correlations in magnitude series to assess nonlinearities: application to multifractal models and heartbeat fluctuations, Phys. Rev. E 96 (2017) 032218.
[17] P. Carpena, M. Gómez-Extremera, C. Carretero-Campos, P. Bernaola-Galván, A.V. Coronado, Spurious results of fluctuation analysis techniques in magnitude and sign correlations, Entropy 19 (2017) 00261.
[18] C.K. Peng, S.V. Buldyrev, A.L. Goldberger, S. Havlin, F. Sciortino, M. Simons, H.E. Stanley, Long-range correlations in nucleotide sequences, Nature 356 (1992) 168–170.
[19] C.K. Peng, S.V. Buldyrev, S. Havlin, M. Simons, H.E. Stanley, A.L. Goldberger, Mosaic organization of DNA nucleotides, Phys. Rev. E 49 (1994) 1685–1689.
[20] J.W. Kantelhardt, E. Koscielny-Bunde, H.H.A. Rego, S. Havlin, A. Bunde, Detecting long-range correlations with detrended fluctuation analysis, Physica A 295 (2001) 441–454.
[21] R.M. Bryce, K.B. Sprague, Revisiting detrended fluctuation analysis, Sci. Rep. 2 (2012) 315.
[22] M. Höll, H. Kantz, The relationship between the detrended fluctuation analysis and the autocorrelation function of a signal, Eur. Phys. J. B 88 (2015) 327.
[23] H.E. Hurst, Long-term storage capacity of reservoirs, Trans. Am. Soc. Civ. Eng. 116 (1951) 770–799.
[24] J.W. Kantelhardt, S.A. Zschiegner, E. Koscielny-Bunde, S. Havlin, A. Bunde, H.E. Stanley, Multifractal detrended fluctuation analysis of nonstationary time series, Physica A 316 (2002) 87–114.
[25] T. Feng Tao, Z.T. Fu, X. Deng, J.Y. Mao, A brief description to different multi-fractal behaviors of daily wind speed records over China, Phys. Lett. A 373 (2009) 4134–4141.
[26] L.H. Gao, Z.T. Fu, Multi-fractal behaviors of relative humidity over China, Atmos. Oceanic Sci. Lett. 6 (2013) 74–78.
[27] N.M. Yuan, Z.T. Fu, J.Y. Mao, Different multi-fractal behaviors of diurnal temperature range over the north and the south of China, Theor. Appl. Climatol. 112 (2013) 673–682.
[28] D. Nian, Z.T. Fu, Extended self-similarity based multi-fractal detrended fluctuation analysis: A novel multi-fractal quantifying method, Commun. Nonlinear Sci. Numer. Simul. 67 (2019) 568–576.
[29] G. Sugihara, M. Casdagli, E. Habjan, D. Hess, G. Holland, P. Dixon, Residual delay maps unveil global patterns of atmospheric nonlinearity and produce improved local forecasts, Proc. Natl. Acad. Sci. 96 (1999) 14 210–14 215.
[30] D.A.S. Patil, B.R. Hunt, J.A. Carton, Identifying low-dimensional nonlinear behavior in atmospheric data, Mon. Weather Rev. 129 (2001) 2116–2125.
[31] I. Bartos, I.M. Jánosi, Atmospheric response function over land: Strong asymmetries in daily temperature fluctuations, Geophys. Res. Lett. 32 (2005) L23820.
[32] B. Gyüre, I. Bartos, I.M. Jánosi, Nonlinear statistics of daily temperature fluctuations reproduced in a laboratory experiment, Phys. Rev. E 76 (2007) 037301.

[33] Y. Ashkenazy, Y. Feliks, H. Gildor, E. Tziperman, Asymmetry of daily temperature records, J. Atmos. Sci. 65 (2008) 3327.
[34] F.H. Xie, Z.T. Fu, L. Piao, J.Y. Mao, Time irreversibility of mean temperature anomaly variations over China, Theor. Appl. Climatol. 123 (2016) 161.
[35] Z.T. Fu, L. Shi, F.H. Xie, L. Piao, Nonlinear features of northern annular mode variability, Physica A 449 (2016) 390–393.
[36] F.H. Xie, D. Nian, Z.T. Fu, Differential temporal asymmetry among different temperature variables' daily fluctuations, Clim. Dyn. (2019) http://dx.doi.org/10.1007/s00382-018-04603-1.
[37] C. Räth, I. Laut, Time series with tailored nonlinearities, Phys. Rev. E 92 (2015) 040902.
[38] C. Räth, M. Gliozzi, I.E. Papadakis, W. Brinkmann, Revisiting algorithms for generating surrogate time series, Phys. Rev. Lett. 109 (2012) 144101.
[39] A. Haluszczynski, I. Laut, H. Modest, C. Räth, Linear and nonlinear market correlations: Characterizing financial crises and portfolio optimization, Phys. Rev. E 96 (2017) 062315.
[40] J. Theiler, S. Eubank, A. Longtin, B. Galdrikian, J. Farmer, Testing for nonlinearity in time series: The method of surrogate data, Physica D 58 (1992) 77–94.
[41] T. Schreiber, A. Schmitz, Improved surrogate data for nonlinearity tests, Phys. Rev. Lett. 77 (1996) 635.
[42] T. Schreiber, A. Schmitz, Surrogate time series, Physica D 142 (2000) 346–382.
[43] H.A. Makse, S. Havlin, M. Schwartz, H.E. Stanley, Method for generating long-range correlations for large systems, Phys. Rev. E 53 (1996) 5445–5449.
[44] R.N. Mantegna, H.E. Stanley, Scaling behaviour in the dynamics of an economic index, Nature 376 (1995) 46.
[45] D.A. Hsieh, Nonlinear dynamics in financial markets: Evidence and implications, Financ. Anal. J. 51 (1995) 55.
[46] S. Ghashghaie, W. Breymann, J. Peinke, P. Talkner, Y. Dodge, Turbulent cascades in foreign exchange markets, Nature 381 (1996) 767.
[47] R.N. Mantegna, H.E. Stanley, Turbulence and financial markets, Nature 383 (1996) 587.
[48] A. Bunde, J.F. Eichner, J.W. Kantelhardt, S. Havlin, Long-term memory: A natural mechanism for the clustering of extreme events and anomalous residual times in climate records, Phys. Rev. Lett. 94 (2005) 04870.
[49] S.M. Osprey, M.H.P. Ambaum, Evidence for the chaotic origin of northern annular mode variability, Geophys. Res. Lett. 38 (2011) L15702.

Please cite this article as: Z. Yu, Y. Huang and Z. Fu, Nonlinear strength quantifier based on phase correlation, Physica A (2019) 123492, https://doi.org/10.1016/j.physa.2019.123492.